Low-temperature specific heat of hydrogen-chemisorbed graphite—alkali-metal intercalation compounds

Toshiaki Enoki
Institute for Molecular Science, Okazaki 444, Japan

Mizuka Sano
Department of Chemistry, Faculty of Science, Kumamoto University, Kumamoto 860, Japan

Hiroo Inokuchi
Institute for Molecular Science, Okazaki 444, Japan
(Received 21 January 1985)

The results of low-temperature specific-heat measurements are presented for hydrogen-chemisorbed C_8M (M=K,Rb), to clarify the effects of dissolved hydrogen on its electronic and lattice vibrational properties. The density of states at the Fermi level is suppressed through a charge transfer from C_8M to hydrogen which is stabilized in interstitial sites in the intercalate layers. This finding is consistent with the results of ESR and positron-annihilation measurements. The introduction of hydrogen increases the acoustic and optic phonon energies for C_8KH_x ($x<0.1$). The electronic effects of dissolved hydrogen are considered to be the cause of the increase. At the hydrogen-saturated concentration ($C_8KH_{2/3}$), the phonon energies are lowered by an increase in the effective mass of the intercalants due to the strong ionic coupling between K and H through bondings with hydrogen. In the case of the C_8Rb system, the acoustic-phonon energies increase while the optic-phonon ones decrease through the introduction of small concentrations of hydrogen ($x<0.1$). The effects of dissolved hydrogen on the superconductivity of C_8KH_x are discussed using the specific-heat results.

I. INTRODUCTION

It is known that graphite—alkali-metal intercalation compounds have catalytic activities for hydrogen leading to occlusion of hydrogen in the intercalate layers of the compounds. At temperatures below about 200 K, the second-stage compounds $C_{24}M$ (M=K, Rb, and Cs) physisorb hydrogen molecules in the vacant sites of alkali-metal atoms in the intercalate layers like molecular sieves. This is because the density of alkali-metal atoms in the second-stage compounds is only $\frac{2}{3}$ that of a two-dimensional, triangular close-packed stacking in the intercalate layers.[1-3] Ortho-para-hydrogen conversion takes place through the physisorption in and/or on the compounds. At higher temperatures, hydrogen is inserted chemisorptively in the intercalate layers where hydrogen molecules are dissociated into atoms.[4-7] Through this process the compounds exhibit activities for the H-D exchange reaction.

Previous phenomenological studies on hydrogen absorption in graphite compounds have revealed phenomena as interesting as those in transition and rare-earth metals such as PdH_x, in spite of the absence of systematical studies on the hydrogen-absorbed graphite compounds. In the case of transition-metal hydrides, the volume of the interstitial sites for the metal atoms is so small that the dissolved hydrogen is greatly affected by the conduction electrons of the transition metal through intimate interactions between the hydrogen and transition-metal atoms, so that the systems are considered to be metal-hydrogen alloys.[8] On the other hand, alkali-metal hydrides such as KH are ionic insulators formed through complete charge transfer (K^+H^-). For hydrogen-chemisorbed graphite—alkali-metal intercalation compounds which contain intercalated alkali-metal—hydride layers, conduction electrons of the graphite compounds will have only a small effect on the absorbed hydrogen, since the volume of the interstitial sites between alkali-metal atoms in the intercalate layers is large. Therefore, hydrogen-chemisorbed graphite—alkali-metal intercalation compounds are expected to have novel properties different from both transition-metal hydrides and alkali-metal hydrides.

In order to clarify the mechanism of hydrogen chemisorption into the graphite compounds and the solid-state properties of hydrogen-absorbed graphite compounds, several studies have been recently carried out. The change in magnetic susceptibilities as a function of hydrogen content has been investigated for hydrogen-chemisorbed C_8K by Furdin *et al.*[9] Conard *et al.* suggested that dissolved hydrogen in C_8K was paramagnetic by means of magnetic resonance studies.[10] We presented a systematic study on hydrogen chemisorption in C_nM (n=8 and 24; M=K, Rb, and Cs) using ESR and electrical conductivity, and showed that the stabilization of absorbed hydrogen species in interstitial sites in the intercalate layers proceeds through the dissociation of hydrogen molecules and subsequent charge transfer from C_nM to hydrogen.[11-13] The dissolved hydrogen in the graphite compounds was revealed to form the hydride ion H^- with a localized character by means of positron-annihilation studies.[14]

Recently, Kaneiwa *et al.* showed that the superconducting transition temperature in C_8K is enhanced by the presence of chemisorbed hydrogen in the intercalate layers.[15,16] It is known that the superconductive behavior of transition metals is strongly influenced by dissolved hydrogen. For example, the transition temperature of PdH_x increases as a function of hydrogen content.[8] The effects of dissolved hydrogen on the superconductivity are thought to originate from changes in the electronic and lattice structure due to hydrogen absorption.[17] The enhancement in T_c for graphite compounds is explained via a different mechanism from that for the change in T_c for transition-metal hydrides. The present authors are interested in the correlation between hydrogen chemisorption and superconductivity in C_8K.

In this paper we investigate the low-temperature specific heat of the hydrogen-chemisorbed first-stage compounds C_8K and C_8Rb in order to clarify the effects of dissolved hydrogen on the electronic and lattice properties and the origin of the superconductivity enhancement of C_8K.

II. EXPERIMENTAL

Samples of C_8K and C_8Rb were prepared from Grafoil GTA (Union Carbide Co.) since Grafoil-based samples chemisorb hydrogen easily, while hydrogen chemisorption in HOPG-based samples is extremely weak (HOPG denotes highly oriented pyrolytic graphite). After Grafoil ground into a 16-mesh powder and alkali-metal vacuum-distilled three times was sealed under vacuum in a glass tube, the reaction to C_8M (M=K or Rb) was carried out at 260°C for about 1 week, following the procedures described in the literature.[18] As C_8M is extremely air-sensitive, the samples were transferred to Au-plated copper sample cells (about 30 g in weight, 16 mm in diameter, and 58 mm in length) in a Dri-Lab glove box (Vacuum/Atmosphere Co.) operated under purified Ar with an impurity level of 1 ppm. The samples were then tightly compacted in the sample cell in order to achieve intimate thermal contact to the wall of the sample cells. The sample cell was sealed by means of an In seal, evacuated through a 1.5-mm-diam copper tube, and then sealed off. The weights of C_8K and C_8Rb were 9.3893 and 12.8151 g, respectively. The packing densities were 0.93 and 1.27 g/cm^3 for C_8K and C_8Rb, respectively. Specific heats were measured using an adiabatic calorimeter from 1.5 to about 10 K, where a calibrated Ge thermometer was used.

After measuring the specific heat of pristine C_8K and C_8Rb, hydrogen, purified by passage through a 450°C heated Pd-Ag thimble, was introduced to the sample cell through the 1.5-mm-diam copper tube. The amount of dissolved hydrogen in C_8M was estimated from a change in hydrogen pressure during the time of hydrogen chemisorption at room temperature. For C_8K, uptake of hydrogen gave $C_8KH_{0.0547}$ at 9.4×10^3 Pa in 80 min and $C_8KH_{0.6485}$ at 9.09×10^4 Pa in a hydrogen-saturated steady state which was achieved in about 1 week. In the case of C_8Rb, $C_8RbH_{0.0546}$ was obtained at 7.95×10^4 Pa in a hydrogen-saturated state in about 1 h, which is consistent with the previous result obtained with a powdered-graphite-based C_8Rb.[6] Specific heats of hydrogen-chemisorbed compounds were measured after evacuation of gaseous hydrogen for about 1 min in order to prevent gaseous hydrogen from contributing to the specific heat. (Desorption of hydrogen was considered to be negligible because of the short pumping time and the small volume of the sample cell.)

III. EXPERIMENTAL RESULTS

Figure 1 shows the temperature dependence of the specific heat for C_8K and for hydrogen-absorbed C_8K, where the molecular weight is defined from the formula unit $CK_{1/8}H_{x/8}$. The C_M/T-versus-T^2 plots deviate from linear dependences above about 4 to 5 K for all samples. This means the specific heats obey the following equation, consistent with the previous results for pristine C_8M (M=K, Rb, and Cs),[19–21]

$$C_M=\gamma T+\alpha T^3+\Delta C_M\ , \tag{1}$$

where the first term is an electronic contribution and the second is due to acoustic phonons. Following the assignment of Suganuma *et al.*,[21] the deviation ΔC_M is associated with low-energy optic phonons, characteristic of the lattice vibrations in the C_8M systems. The temperature dependence of the contribution of optic phonons, ΔC_M, in the higher-temperature region (to about 10 K) is shown in Fig. 2. Judging from the results, ΔC_M was found to obey the following equation,

$$\Delta C_M=N_A k_B n\left[\frac{T_E}{T}\right]^2\exp\left[-\frac{T_E}{T}\right], \tag{2}$$

where N_A is Avogadoro's number, T_E the Einstein characteristic temperature for optic phonons, and n the number of degrees of freedom for the optic phonons. Equation (2) is an approximate formula for the contribution from Einstein lattice vibrations for $T\ll T_E$.

Figure 3 shows the temperature dependence of the specific heat for C_8Rb and hydrogen-absorbed C_8Rb. For both C_8Rb and $C_8RbH_{0.0546}$, as well as for C_8K, the

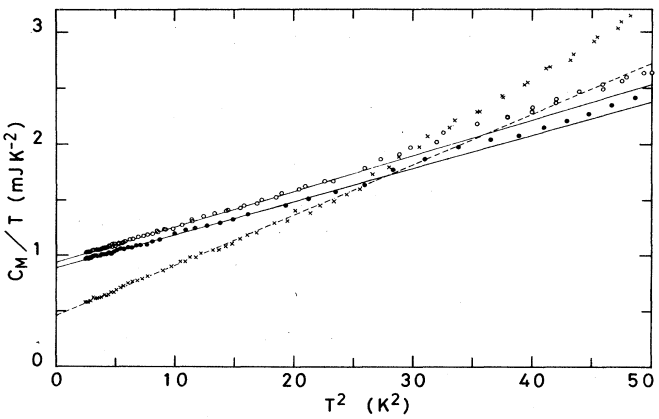

FIG. 1. C_M/T-vs-T^2 plots for C_8K and hydrogen-absorbed C_8K. Open circles denote the result of C_8K, solid circles $C_8KH_{0.0547}$, and crosses $C_8KH_{0.6485}$. Solid and dashed lines were obtained by means of the method of least squares.

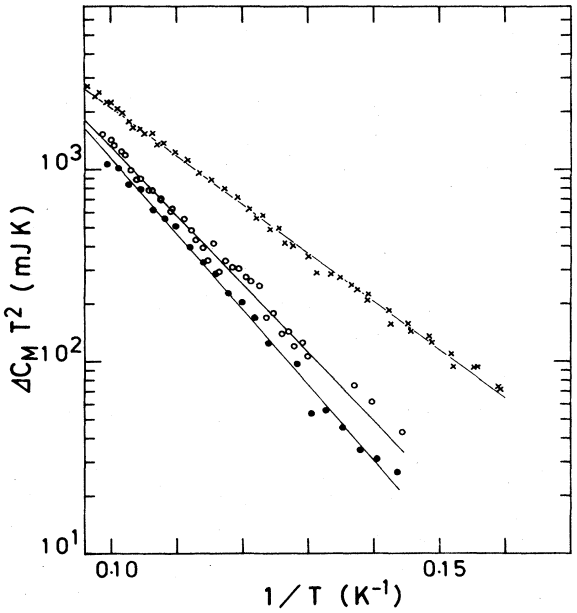

FIG. 2. $\Delta C_M T^2$-vs-$1/T$ plots for C_8K and hydrogen-absorbed C_8K. Open circles denote the result of C_8K, solid circles $C_8KH_{0.0547}$, and crosses $C_8KH_{0.6485}$. Solid lines were obtained by means of the method of least squares.

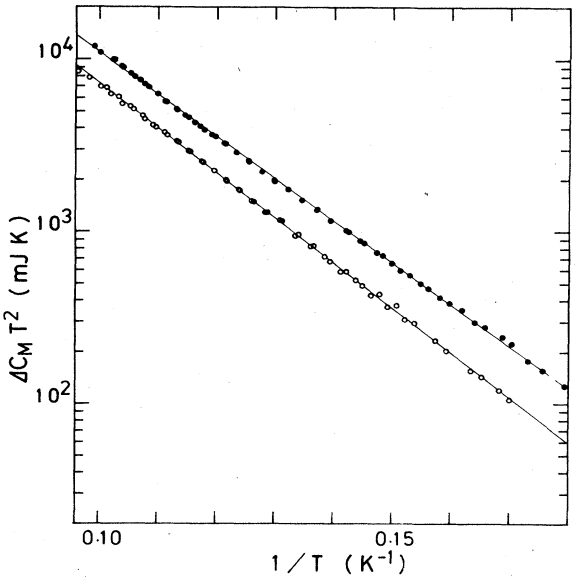

FIG. 4. $\Delta C_M T^2$-vs-$1/T$ plots for C_8Rb and hydrogen-absorbed C_8Rb. Open circles denote the result of C_8Rb, and solid circles $C_8RbH_{0.0546}$. Solid lines were obtained by means of the method of least squares.

specific heat obeys Eq. (1). That of C_8Rb shows a deviation from a linear dependence of C_M/T on T^2 above about 4 to 5 K, while the deviation was observed above about 3 to 4 K for hydrogen-absorbed C_8Rb. The deviations due to optic phonons for the C_8Rb system were found to be larger than those for C_8K. The temperature dependence of the contribution of optic phonons, ΔC_M, in the higher-temperature region (to about 10 K) is shown in Fig. 4, where fairly good agreement is obtained between the experimental results and Eq. (2). Tables I and II summarize the specific-heat parameters for the electronic and lattice contributions of both the C_8K and C_8Rb systems, respectively.

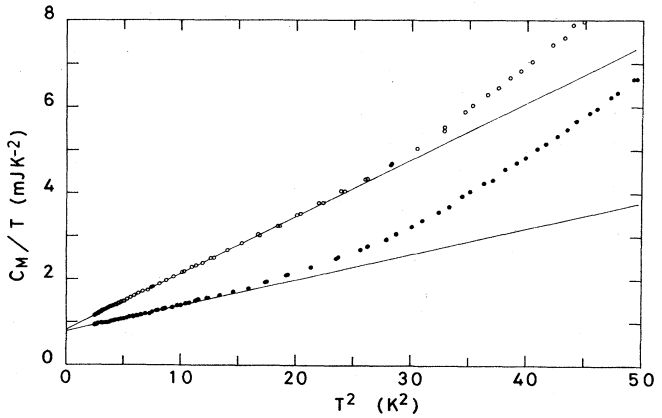

FIG. 3. C_M/T-vs-T^2 plots for C_8Rb and hydrogen-absorbed C_8Rb. Open circles denote the result of C_8Rb, and solid circles $C_8KH_{0.0546}$. Solid lines were obtained by means of the method of least squares.

IV. DISCUSSION

A. Comparison with the previous specific-heat measurement results for pristine C_8K and C_8Rb

Although the qualitative properties of the present results for Grafoil-based C_8K and C_8Rb samples are consistent with the previous ones, there are differences in the parameters for the electronic and lattice contributions.[19–21] In the case of C_8K, the present result of the electronic specific-heat coefficient $\gamma=0.94$ mJ/K^2 mol is larger than the results for the powdered-graphite-based sample (0.784 mJ/K^2 mol) (Ref. 19) and the HOPG-based one (0.84 mJ/K^2 mol) (Ref. 20) while, for C_8Rb, the present value $\gamma=0.82$ mJ/K^2 mol is between the powdered-graphite-based one (0.727 mJ/K^2 mol) (Ref. 21) and the HOPG-based one (1.3 mJ/K^2 mol) (Ref. 20). Judging from both the present result and that for graphite powder,[19,21] the electronic specific-heat coefficient γ decreases in the order of K, Rb, and Cs among C_8M

TABLE I. Electronic specific heat. The density of states at E_F, $N(E_F)$, is estimated with electron-phonon coupling parameter $\lambda=0$.

	γ (mJ/K^2 mol)	$N(E_F)$ (states/eV atom of C)
C_8K	0.94±0.01	0.40
$C_8KH_{0.0547}$	0.89±0.01	0.38
$C_8KH_{0.6485}$	0.46±0.01	0.20
C_8Rb	0.82±0.01	0.35
$C_8RbH_{0.0546}$	0.78±0.01	0.33

TABLE II. Lattice specific heat. The number of degrees of freedom, n, for the optic-phonon modes is estimated for one mole of C, and n_M is estimated for one mole of alkali-metal atom.

	Θ_D (K)	T_E (K)	n (n_M)
C_8K	393.5	82.2	0.087 (0.70)
$C_8KH_{0.0547}$	403.0	90.7	0.146 (1.17)
$C_8KH_{0.6485}$	350.3	58.1	0.025 (0.20)
C_8Rb	245.4	60.3	0.100 (0.80)
$C_8RbH_{0.0546}$	319.1	56.2	0.115 (0.92)

(M=K, Rb, and Cs), though we have an exception for the HOPG-based C_8Rb sample due to the difference in the nature of the parent graphite and the experimental conditions among the three kinds of experiments. Theoretical and experimental studies[22–26] on the electronic structure of the first-stage compounds C_8M show that the basic nature of the electronic structure is independent of the sort of alkali metals among K, Rb, and Cs, and the alkali-metal atoms have a fractional charge due to a degeneracy of both graphitic π^* and alkali-metal s bands. Ionization potentials I_P of K, Rb, and Cs metals are 4.339, 4.176, and 3.893 eV, respectively. This means that the tendency to become positively charged is on the order of Cs > Rb > K. The amount of positive charge on the alkali-metal atom has a reverse correlation to the contribution to γ of an alkali-metal s band.[22,23] The experimental results for γ are consistent with the tendency depending on the value of I_P. The fact that the activity for hydrogen chemisorption is in the order of $C_8K > C_8Rb > C_8Cs$ (Ref. 12) is easily explained by this difference in the electropositivity because the more positive the alkali-metal atom, the more stable the graphitic compound that is formed and the less active the sample for further hydrogen chemisorption.

The present result of the Debye temperature for C_8K, Θ_D=393.5 K, is larger than the results of the powdered-graphite-based sample (Θ_D=234.8 K) and the HOPG-based one (Θ_D=374 K), but the difference between the present and the HOPG-based ones is rather small. In the case of C_8Rb, the present value Θ_D=245.4 K is smaller than the previous two experiments (Θ_D=361.9 K for the powdered-graphite-based one and 439 K for the HOPG-based one). The present results for the contribution of the acoustic phonons reveal that Θ_D is proportional to $1/\sqrt{m}$ with an accuracy of 8%, where m is the atomic weight of alkali metal (m=39.102 for K and 85.4678 for Rb), consistent with the neutron scattering results of the phonon dispersion.[27] This finding suggests that the acoustic phonons are due to the C-intercalant-C composite layers, even for the first-stage compounds, as well as those for the higher-stage compounds.[21,28]

In our results, the Einstein characteristic temperatures T_E are 82.2 and 60.3 K for C_8K and C_8Rb, where the results of C_8K are unique (see Table II). The present value of C_8Rb is smaller than the values from the previous experiments (T_E=71 K for the powdered-graphite-based sample and 65 K for the HOPG-based sample). In the case of the optic-phonon mode, which is identified with the two-dimensional vibrations in the plane of the alkali-metal atoms,[21,28,29] we find a $1/\sqrt{m}$ dependence of T_E with an accuracy of 8%, though the observed values are a little smaller than the values predicted by a theoretical study, where T_E=145 K for C_8K and 105 K for C_8Rb.[29]

As those vibrational modes are two dimensional, the number of degrees of freedom of these modes, n_M, should be 2 for each alkali-metal atom unless this freedom is quenched.[21] On the other hand, the degrees of freedom n_M observed for C_8K and C_8Rb are 0.70 and 0.80, respectively, as shown in Table II, which are significantly smaller than 2. Alkali-metal atoms form a two-dimensional triangular lattice in the intercalant layers for first-stage compounds, while the intraplane density of alkali-metal atoms is $\frac{2}{3}$ of that of first-stage ones in the case of higher-stage ones where the number of degree of freedom is around 2.[21] Judging from the experimental results showing a small number for the degrees of freedom, and lower vibrational energies than the theoretically predicted ones,[29] strong interactions between alkali-metal atoms associated with the high intraplane density of alkali-metal atoms might induce clustering among them in the first-stage compounds. The diameters of alkali-metal atoms with a partial charge in C_8K and C_8Rb are 3.40 and 3.64 Å for K and Rb, respectively, which are smaller than 4.92 Å, the periodicity of the 2×2 triangular alkali-metal superlattice relative to the graphitic layer.[12] The clustering can be explained with the inconsistency between the diameter and the lattice periodicity.

B. Effects of dissolved hydrogen in C_8K and C_8Rb

Figure 5 shows the change in the electronic specific-heat coefficient γ depending on the content of dissolved hydrogen in C_8M. γ decreases monotonically in C_8KH_x, as the dissolved hydrogen concentration x increases, i.e., the decrement in γ is 5.3% at x=0.0546, and 51.1% at x=0.6485, where the content of absorbed hydrogen is saturated. (Colin and Hérold estimated that the concentration at the saturation limit was $\frac{2}{3}$.[6]) In the case of C_8K, hydrogen is introduced in interstitial sites for alkali-metal atoms with a two-dimensional close-packed triangular lattice in the intercalate layers of the first-stage structure for $x<0.1$, and then, above x=0.1, a greater amount of dissolved hydrogen induces a structure change to a second-stage compound where bilayers of K atoms between which H atoms are inserted are intercalated between two graphitic bilayers.[4,6,7,9,12] The C_8KH_x system is a mixture of the first-stage and the second-stage structures in the concentration region $0.1<x<\frac{2}{3}$. Finally, the homogeneous second-stage structure is completed at the hydrogen-saturated concentration $x=\frac{2}{3}$.

Since hydrogen has a large electron affinity in metallic materials (the H 1s is at 13.6 eV below the vacuum level), a charge transfer takes place from C_8M to H after the introduction of hydrogen, mentioned in the previous results of ESR and positron-annihilation experiments.[11–14] This behavior is similar to that of transition-metal hydrides, where, generally speaking, the generation of bonding orbi-

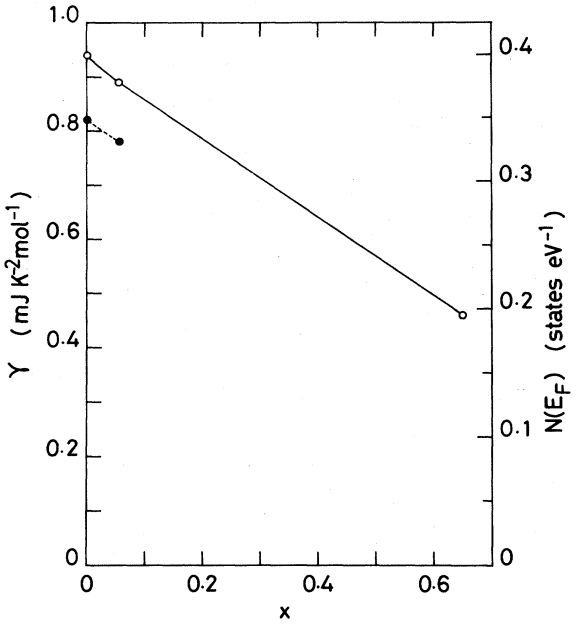

FIG. 5. The hydrogen concentration dependence of γ and $N(E_F)$ for C_8KH_x and C_8RbH_x. Open circles denote the results of C_8KH_x and solid circles C_8RbH_x. Solid and dashed lines are guides for the eye. $N(E_F)$ is not corrected for λ.

tals between hydrogen and transition-metal atoms and hydrogen atoms around 5 eV below the Fermi level causes a decrease of the density of states at the Fermi level.[8] Judging from the electronic structure of C_8K,[22,23] the decrease in the electronic density of states at the Fermi level, $N(E_F)$, as a function of x, is caused by the lowering of the Fermi level E_F due to a donation of C_8K electrons to H near E_F. Therefore, hydrogen dissolved through the chemisorption process is stabilized as hydride ions H^- with negative charges. The fact that $N(E_F)$ has a continuous change as a function of x in spite of the existence of a structure change at $x\sim 0.1$ suggests that the electronic structure of hydrogen-absorbed C_8K with the second-stage structure ($x>0.1$) is similar to that of the first-stage C_8KH_x ($x<0.1$).

Here, we estimate the charge-transfer rate from a donor K atom, following the rigid-band model by Sugihara.[30] Taking into account that hydrogen atoms are stabilized as hydride ions H^- in the high-hydrogen-concentration region, we can adopt a formula $C_8^{-f(1-x)/8}K^{+f}{}_{(1-x)}(K^+H^-)_x$ for C_8KH_x, where f is the charge-transfer rate per K atom. The number of electrons n_C transferred to carbon atoms from potassium atoms per unit volume is given as follows,

$$n_C=n_U f(1-x)=\int_0^{E_F} dE\, D_G(E)\ , \tag{3}$$

where $D_G(E)$ is a partial density of states attributable to graphitic electrons and n_U is the number of unit cells per unit volume, while the number of electrons n_K on potassium sites per unit volume is

$$n_K=n_U(1-f)(1-x)=\int_0^{E_F(s)} dE\, D_s(E)\ , \tag{4}$$

where $D_s(E)$ is the partial density of states attributable to the K $4s$ band and E is measured from the bottom of the s band. The partial densities of states for the two-dimensional graphitic band and the three-dimensional s band are described in the following way, respectively:

$$D_G(E)=\frac{8E}{\pi I_c A^2}\ , \tag{5}$$

and

$$D_s(E)=\frac{1}{\pi^2}\left[\frac{2m^*}{\hbar^2}\right]^{3/2}\sqrt{E}\ , \tag{6}$$

where $E(k)=Ak$ for the graphitic π-electron energy and $E(k)=\hbar^2k^2/2m^*$ for the s-electron energy. If we neglect π-s mixing, we can get the total density of states per atom of C at E_F by means of Eqs. (3)—(6),

$$N(E_F)=\frac{3^{1/4}a}{(2\pi)^{1/2}A}f^{1/2}(1-x)^{1/2}+\frac{9^{1/3}m^*a^{4/3}I_c^{2/3}}{2^{1/3}(2\pi)^{4/3}\hbar^2}(1-f)^{1/3}(1-x)^{1/3}\ , \tag{7}$$

where a is the in-plane lattice constant and I_c is the c-axis repeat distance. Since the parameters A and m^* in Eq. (7) are not available for estimating the charge transfer rate f, we modify (7) as follows,

$$N(E_F)=uf^{1/2}(1-x)^{1/2}+v(1-f)^{1/3}(1-x)^{1/3}\ . \tag{8}$$

If we use theoretical results for the ratio of the partial densities of states,[22,23] and normalize the resulting value to the present experimental results, and use $f=0.6$ for C_8K ($x=0$), u and v are numerically estimated to be 0.324 and 0.199, respectively. (The present discussion neglects a correction for electron-phonon coupling parameter λ.) In the case of $C_8KH_{0.6485}$, if we adopt $f=1.0$ and neglect the effect of the structure change, we get $N(E_F)=0.19$ states/eV atom of C, which is in good agreement with the observed value, 0.20 states/eV atom of C. This finding suggests that the charge transfer to hydrogen causes the change in the valence of K from a partial positive value of $+0.6$ to $+1$. Through this charge transfer by hydrogen uptake, the distributions of electrons on K, C, and H atoms are changed as follows: $0.4e$ for K and $0.075e$ for C in C_4K, and $0e$ for K, $0.044e$ for C, and $1e$ for H in $C_8KH_{0.6485}$. Moreover, if we adopt the density of states obtained by Inoshita *et al.*[22] to C_8KH_x ($x=0.6485$) and neglect effects due to structural changes, then a 51% decrement in $N(E_F)$ corresponds to transfer of 52% of donor electrons in C_8K to hydrogen. The second-stage structure of C_8KH_x with intercalated K-H-K composite layers is considered to be stabilized through the gain of lattice energy among the K^+ and H^- ions generated by the charge transfer. The slope of an $N(E_F)$-versus-x plot, $dN(E_F)/dx$, is estimated to be -0.31 states/eV mol atom of H from Fig. 5, so that $N(E_F)$ will be 0 at about $x=1.3$. This suggests that a formation of ionic K^+-H^- intercalants in the intercalate layers tends to reduce the charge-transfer process between graphite and intercalant, due to the large electron affinity of hydrogen.

In the case of C_8Rb, γ also decreases through the uptake of hydrogen. The decrement in γ is 4.9% at $x=0.0546$, which is the concentration of the saturation limit at ambient pressure. Since the decrement $[dN(E_F)/dx = -0.31$ states/eV mol atom of H] is similar to that for $C_8KH_{0.0547}$, dissolved hydrogen is suggested to have similar charge-transfer effects on the electronic structure for both C_8K and C_8Rb. The previous ESR experiment on C_8Rb showed the generation of hydrogen species with localized spins.[12] Therefore, chemisorbed hydrogen is stabilized as $H^{\delta-}$.

Figure 6 shows the hydrogen-concentration dependence of the Debye temperatures Θ_D for the acoustic-phonon modes and the Einstein characteristic temperatures T_E for the optic-phonon modes. Figure 7 presents the number of degrees of freedom n (or n_M) for the optic-phonons. In the case of C_8KH_x, Θ_D is increased as a function of x within the concentration range ($x<0.1$) where introduction of hydrogen does not cause a structure change. At $x=0.6485$, where the structure is the second-stage one, Θ_D decreases by 11%. T_E increases by 10% and the number of degrees of freedom, n, increases by 17% as a function x at $x=0.0547$, while the former and the latter decrease by 29% and 71%, respectively, at the hydrogen-saturated concentration $x=0.6485$.

In the case of transition-metal hydrides,[8] introduction of hydrogen in interstitial sites in a metal-atom lattice causes a lattice expansion because the size of dissolved hydrogen species (~ 2.9 Å^3) is too large to be accommodated in the interstitial sites. The lattice expansion reduces the lattice vibrational energies. On the other hand, hydrogen atoms dissolved in metal have electronic interactions to the metal atoms, and chemical bonds are generated between hydrogen and metal atoms. This enhances the lattice vibrational energies. The spectra of lattice vibrational energies are modified through the competition between the lattice expansion and the electronic effects for transition-metal hydrides. Moreover, the optic-phonon modes due to the dissolved hydrogen atoms have frequencies around 1000 cm^{-1}. For palladium hydride, hydrogen loading causes a lowering of the lattice vibrational energies, while vibrational energies in Nb, Ta, and V tend to increase through the electronic effects due to hydrogen.[8]

As to the C_8K system, hydrogen uptake induces a charge transfer from C_8K to hydrogen as discussed above, and then generates chemical bonding between C_8K and hydrogen which is considered to be fairly weak in comparison with the bondings in transition-metal hydrides, because the volume of interstitial sites in C_8K is large enough to accommodate hydrogen atoms. The lattice expansion due to the uptake of hydrogen is negligible, taking into account this large volume of the interstitial sites. Moreover, the decrease of electrons in antibonding graphitic π^* orbitals through the charge transfer to hydrogen will restore the vibrational energies of graphite. Therefore, for $C_8KH_{0.0547}$, where the first-stage structure is conserved in spite of hydrogen uptake, small increases in the energies of the acoustic- and the optic-phonon modes shown here are thought to be governed by the electronic effects which are relatively small compared with those in

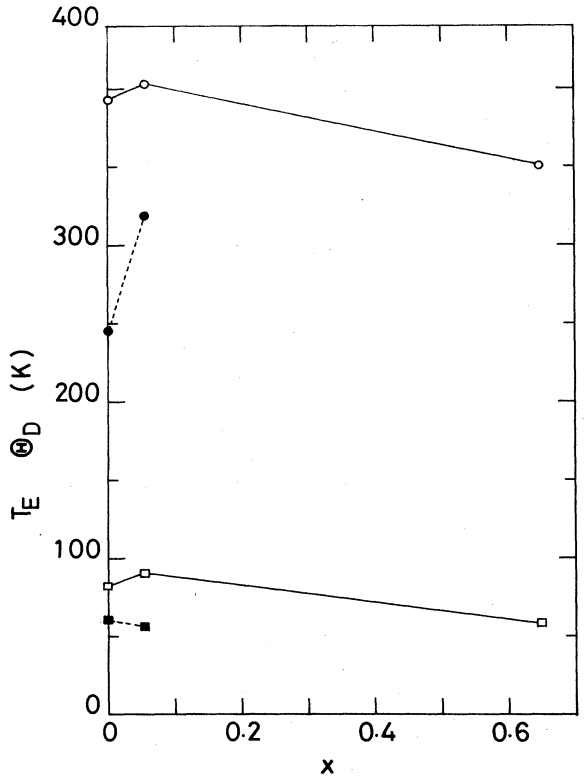

FIG. 6. The hydrogen concentration dependence of Θ_D and T_E for C_8KH_x and C_8RbH_x. Open and solid circles denote Θ_D for C_8KH_x and C_8RbH_x, respectively, and open and solid squares T_E for C_8KH_x and C_8RbH_x, respectively. Solid and dashed lines are guides for the eye.

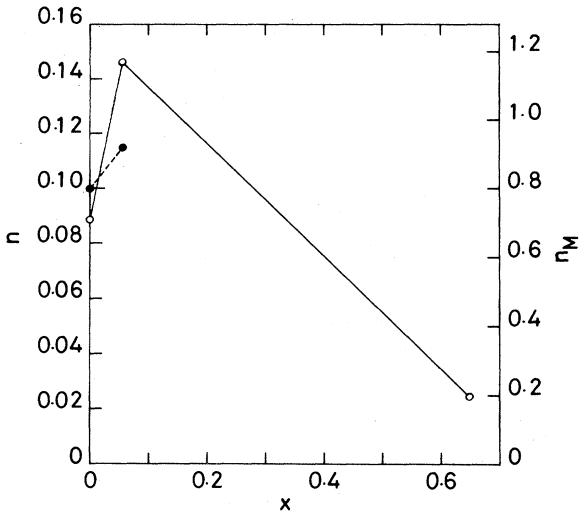

FIG. 7. The number of degrees of freedom as a function of hydrogen concentration x for the optic-phonon modes. n denotes the degree of freedom per atom of C and n_M per atom of alkali-metal atoms. Open circles are for a C_8K system and solid circles for a C_8Rb one. Solid and dashed lines are guides for the eye.

transition-metal hydrides.

As mentioned in subsection A, alkali-metal atoms have clustering in the intercalate layers through a small incommensuration between the periodicity of the triangular lattice of alkali-metal atoms and the diameter of alkali-metal atoms. Insertion of hydrogen atoms in the interstitial sites among alkali-metal atoms will break the clustering among alkali-metal atoms. The restoration of the degrees of freedom in the two-dimensional vibrations in the plane of the alkali-metal atoms shown for $C_8KH_{0.0547}$ in Fig. 7 is caused by the dissolution of the clustering.

In the hydrogen-saturated compound $C_8KH_{0.6485}$ with the second-stage structure, hydride ions H^- are surrounded by K cations whose positive charge increases by a large amount through the charge transfer from C_8K to H, located in intercalant layers sandwiched between double graphitic layers. The strong ionic interactions in the intercalant composite K^+-H^--K^+ layers will reduce the effective mass of intercalants not only for the acoustic vibration of C-intercalant-C but also for the optic vibration of the two-dimensional intercalant plane. This is suggested by the experimental facts, the decreases of Θ_D for the acoustic-phonon modes, and T_E and the number of degrees of freedom n_M for the optic-phonon modes, as shown in Figs. 6 and 7. The finding that n_M is only $\frac{1}{10}$ of the number of degrees of freedom in the two-dimensional vibration for the hydrogen-saturated concentration means that there is considerable development of the clustering in the intercalant layers.

In the case of the C_8Rb system, Θ_D increases by 30%, T_E decreases by 7%, and n_M increases by 15% for $x=0.0546$. For C_8K, the volume of an interstitial site among K atoms is so large in comparison with the small diameter of the K atoms that hydrogen insertion might not require a lattice expansion, while one of the reasons for the inactivity for hydrogen occlusion in C_8Cs is considered to come from the small volume for an interstitial site between the large Cs atoms.[12] Introduction of hydrogen will have a larger effect on the lattice expansion in C_8Rb than in C_8K, because of the larger size of the Rb atoms. A large increase in Θ_D for the acoustic-phonon mode and a small decrease in T_E for the optic-phonon mode suggest nonuniform change in lattice energies which is determined by a subtle competition between the electronic effects and the lattice expansion for the C_8Rb system. The increase in the number of degrees of freedom for the optic-phonon modes for $C_8RbH_{0.0546}$ also provides evidence for the elimination of clustering among Rb atoms through the generation of weak bonding with hydrogen atoms.

C. Superconductivity in hydrogen-absorbed C_8K and C_8Rb systems

The effects of dissolved hydrogen on superconductivity have been investigated for the C_8K system by Kaneiwa *et al.* and Sano *et al.*[15,16] For $C_8KH_{0.19}$ prepared from HOPG, the superconducting transition temperature T_c was enhanced to 0.22 K from 0.15 K of C_8K,[31–35] while T_c was not able to be observed down to 0.05 K for a hydrogen-saturated sample $C_8KH_{2/3}$ (see Fig. 8). Following BCS theory, T_c is given as follows,

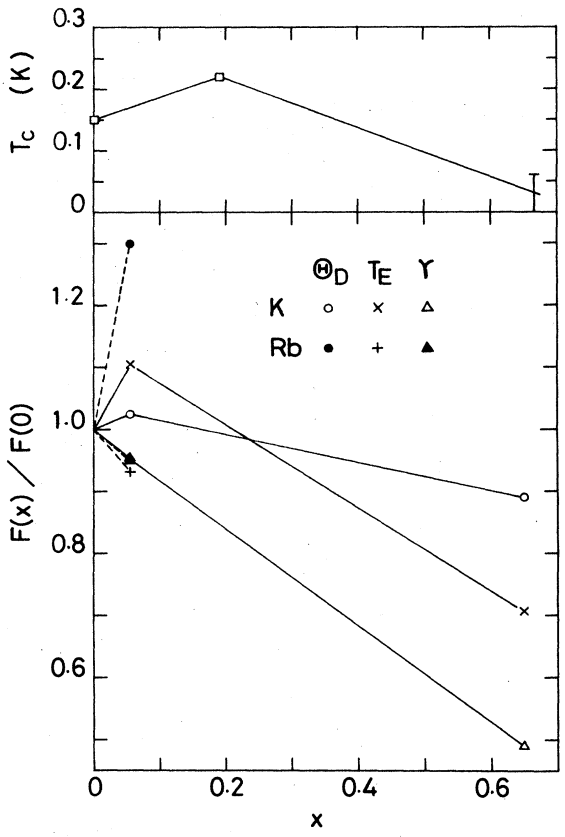

FIG. 8. The change in specific-heat parameters Θ_D, T_E, and γ as a function of hydrogen concentration x. Θ_D, T_E, and γ are denoted by ○, ×, and △, respectively, for the C_8K system, while those by ●, +, and ▲, respectively, are for the C_8Rb system. The change in the superconducting transition temperature T_c (□) is also shown after the literature (Refs. 15 and 16). Solid and dashed lines are guides for the eye.

$$T_c = 0.85\Theta_D \exp[-1/N(E_F)V] , \tag{9}$$

where V is an effective electron-electron attractive interaction generated through electron-phonon interactions. Using the McMillan equation,[36] the electron-phonon coupling parameter λ is related to T_c in the following way,

$$T_c = \frac{\Theta_D}{1.45} \exp\left[-\frac{1.04(1+\lambda)}{\lambda-\mu^*(1+0.62\lambda)} \right] , \tag{10}$$

where μ^* is the Coulomb repulsive constant (assumed to be 0.1). The density of states corrected for λ, $N(E_F)^0$, is given by the following equation,

$$\gamma = \tfrac{1}{3}\pi^2 k_B^2 (1+\lambda) N(E_F)^0 . \tag{11}$$

For $C_8KH_{0.19}$, the system is a mixture of the first-stage and the second-stage hydrogen-absorbed C_8K structures, $C_8KH_{0.1}$ and $C_8KH_{2/3}$, with a ratio of $[C_8KH_{0.1}]/[C_8KH_{2/3}] \sim 4$, since the concentration $x=0.19$ occurs in an inhomogeneous structure region.[9] X-ray measurement of the HOPG-based $C_8KH_{0.19}$ sample used for the super-

conductivity measurement suggests the coexistence of the diffraction patterns for both the first- and the second-stage structures with the expected ratio.[16,37] Taking into consideration that T_c of the saturated hydrogen-absorbed C_8K with a complete second-stage structure, $C_8KH_{2/3}$, is unobservably low,[15] the enhanced T_c for $C_8KH_{0.19}$ is considered to be attributable to the part of the hydrogen-absorbed C_8K with a first-stage structure which contains dissolved hydrogen with $x \sim 0.1$. Hydrogen uptake causes a decrease in the electronic specific-heat coefficient γ and an increase in the Debye temperature Θ_D for C_8KH_x ($x < 0.1$). Following Eq. (9), the former reduces T_c while the lattice enhances it. For $C_8KH_{0.0547}$, T_c is expected to be about 0.19 K by means of an interpolation between 0.15 K for $x=0$ and 0.22 K for $x=0.10$, since the concentration $x=0.0547$ is in the homogeneous structure region. Using Eqs. (9) and (10), we obtain the parameters of superconductivity for hydrogen-absorbed C_8K, where $T_c=0.19$ K is adopted for $x=0.0547$, as well as those for the pristine C_8K and C_8Rb,[38] as shown in Table III. The electron-phonon coupling parameter λ in $C_8KH_{0.547}$ is enhanced by about 2% in comparison with that in the pristine C_8K. In addition to the increase in Θ_D, this enhancement in λ is considered to play an essential role for the increase in T_c and to overwhelm the decrease in $N(E_F)$. For the superconductivity of the C_8K system, it is also possible that the optic-phonon mode might play a role,[39] and, in that case, the increase in T_E for $C_8KH_{0.0547}$ will be favorable to enhance the superconductivity.

Introduction of hydrogen in the interstitial sites induces a charge transfer to form hydride ions $H^{-\delta}$ and to make the K valence more positive. Then, a conduction electron will deform the positive K lattice more for the hydrogen-absorbed C_8K than for pristine C_8K because of the enhancement in interaction between a conduction electron and a $K^{+\delta'}$ atom. A polarization inherent in the $H^{-\delta}$-$K^{+\delta'}$ vibrations will enhance the effective electron-electron attractive interaction, as suggested by the present result.

In the case of the hydrogen-saturated compound $C_8KH_{2/3}$, T_c is suppressed greatly. The estimated value of $\lambda=0.87$ shown in Table III is obtained from the present specific-heat result and the ESR result.[12] This value for λ is too large in comparison with $\lambda=0.30$ for C_8K with weak coupling. This value might have some error since the estimation of the ESR intensity is ambiguous because of the Dysonian line shape of the ESR spectra. As described in subsection B, $C_8KH_{2/3}$ does not have any contributions for conduction electrons from the potassium $4s$ band, since the large electron affinity of hydrogen induces charge transfer from potassium, leading to a change in the charge-transfer rate f of 1. Theoretical study suggests that the superconductivity of the graphite—alkali-metal intercalation compounds is based on the cooperation of graphitic π-band and alkali-metal s-band electrons.[40] Therefore, the absence of superconductivity is considered to be caused by the absence of s-band electrons. The large decrease in the vibrational energies of Θ_D and T_E is also disadvantageous for superconductivity.

Recently, superconductivity of C_8Rb was found at 0.026 K.[38] The lower T_c for C_8Rb than that for C_8K is caused by smaller values of $N(E_F)$, Θ_D, and λ. $\lambda=0.27$ suggests that C_8Rb is a weak-coupling superconductor, similar to C_8K.[31,32] As the present experiment shows a large increase in Θ_D by hydrogen uptake, T_c is expected to be significantly increased for $C_8RbH_{0.05}$, taking into account the discussion of the C_8K system given above.

TABLE III. The parameters of superconductivity, $N(E_F)^0$ is the density of states corrected for electron-phonon interaction.

	T_c (K)	$N(E_F)^0$ (states/eV atom of C)	λ	$N(E_F)^0V$
C_8K	0.15	0.31	0.30	0.13
$C_8KH_{0.0547}$	0.19[a]	0.29	0.31	0.13
$C_8KH_{0.6485}$	<0.05	0.10	0.87	
C_8Rb	0.026	0.28	0.27	0.11

[a]This value is expected from $T_c=0.22$ K for $C_8KH_{0.19}$.

V. SUMMARY

Low-temperature specific heats have been investigated for the hydrogen-chemisorbed C_8K and C_8Rb systems in order to clarify the effects of dissolved hydrogen on their electronic and lattice vibrational properties.

The electronic densities of states at the Fermi level, $N(E_F)$, decrease as a function of dissolved hydrogen concentration for both C_8K and C_8Rb systems. As the energy level of hydrogen $1s$ is far below E_F for C_8M (M=K,Rb), the hydride ion $H^{-\delta}$ is generated and stabilized in the intercalate layers through a charge transfer from C_8M to hydrogen. The decrease in $N(E_F)$ is explained by the charge transfer, consistent with results of ESR and positron annihilation.[11–14]

Two kinds of phonon modes contribute to the low-temperature specific heats for the hydrogen-absorbed systems, as well as those for pristine C_8K and C_8Rb.[19–21] In the case of the C_8K system, the energies of acoustic-phonon modes due to the C-intercalant-C composite layers and optic-phonon modes due to the two-dimensional vibrations in the intercalant planes increase because of the electronic effects of the dissolved hydrogen, under introduction of hydrogen for $x<0.1$, where the hydrogen atoms are dissolved in the intercalate layers of the first-stage structure. In the hydrogen-saturated compound $C_8KH_{2/3}$, which has an intercalant composite layer K^+-H^--K^+ sandwich between two graphitic bilayers, the phonon energies decrease by means of an increase in effective mass of the intercalants due to the strong ionic coupling between K^+ and H^-. For the C_8Rb system, hydrogen uptake raises the acoustic-phonon energy while it lowers the optic-phonon energy. This nonuniform change in vibrational energies is suggested by subtle effects determined by a competition between the electronic effects and the lattice expansion due to dissolved hydrogen since an Rb atom is bigger than a K atom.

From the experimental specific-heat results, the enhancement in superconductivity for the hydrogen-absorbed compound $C_8KH_{0.19}$ is explained by an increase in electron-phonon interaction due to the charge transfer and the polarization inherent to $K^{+\delta'}$-$H^{-\delta}$ vibrations.

The suppression of T_c for the hydrogen-saturated compound $C_8KH_{2/3}$ is caused by the absence of electrons in the potassium s band and the lower vibrational energies.

ACKNOWLEDGMENTS

The authors would like to thank to Dr. K. Sugihara, Dr. G. Roth, Professor M. S. Dresselhaus, Dr. G. Dresselhaus, Dr. M. Kobayashi, and Professor K. Nasu for helpful discussions. They are grateful to Professor U. Mizutani for his advice on specific-heat measurements. This work was supported by the Grant-In-aid in Special Project Research on the Properties of Molecular Assemblies (No. 59112004) from the Ministry of Education, Science and Culture, Japan.

[1]K. Watanabe, M. Soma, T. Onishi, and K. Tamaru, Nature (London) **233**, 160 (1971).
[2]P. Lagrange, A. Metrot, and A. Hérold, C. R. Acad. Sci. **275**, C765 (1972).
[3]K. Watanabe, T.Kondow, M. Soma, T. Onishi, and K. Tamaru, Proc. R. Soc. London, Ser. A **333**, 51 (1973).
[4]D. Saehr and A. Hérold, Bull. Soc. Chim. Fr. **1965**, 3130.
[5]H. Inokuchi, N. Wakayama, T. Kondow, and Y. Mori, J. Chem. Phys. **46**, 837 (1967).
[6]M. Colin and A. Hérold, Bull. Soc. Chim. Fr. **1971**, 1982.
[7]P. Lagrange, A. Metrot, and A. Hérold, C. R. Acad. Sci. **278**, C701 (1974).
[8]G. Alefeld and J. Völkl, *Hydrogen in Metals* (Springer, Berlin, 1978).
[9]G. Furdin, P. Lagrange, A. Hérold, and C. Zeller, C. R. Acad. Sci. **282**, C563 (1976).
[10]J. Conard, H. Estrade-Szwarckoph, P. Lauginie, M. El Markrini, P. Lagrange, and D. Guérard, Synth. Met. **2**, 261 (1980).
[11]T. Enoki, H. Inokuchi, and M. Sano, Chem. Phys. Lett. **86**, 285 (1982).
[12]T. Enoki, M. Sano, and H. Inokuchi, J. Chem. Phys. **78**, 2017 (1983).
[13]T. Enoki, M. Sano, and H. Inokuchi, Mol. Cryst. Liq. Cryst. **96**, 401 (1983).
[14]H. Murakami, M. Sano, I. Kanazawa, T. Enoki, T. Kurihara, Y. Sakurai, and H. Inokuchi, J. Chem. Phys. **85**, 4728 (1985)
[15]M. Sano, H. Inokuchi, M. Kobayashi, S. Kaneiwa, and I. Tsujikawa, J. Chem. Phys. **72**, 3840 (1980).
[16]S. Kaneiwa, M. Kobayashi, and I. Tsujikawa, J. Phys. Soc. Jpn. **51**, 2375 (1982).
[17]M. Gupta, Solid State Commun. **50**, 439 (1984).
[18]D. E. Nixon and G. S. Parry, J. Phys. D **1**, 291 (1968).
[19]U. Mizutani, T. Kondow, and T. B. Massalski, Phys. Rev. B **17**, 3165 (1978).
[20]M. G. Alexander, D. P. Goshorn, and D. G. Onn, Phys. Rev. B **22**, 4535 (1980).
[21]M. Suganuma, T. Kondow, and U. Mizutani, Phys. Rev. B **23**, 706 (1981).
[22]T. Inoshita, K. Nakao, and H. Kamimura, J. Phys. Soc. Jpn. **43**, 1237 (1977).
[23]T. Ohno, K. Nakao, and H. Kamimura, J. Phys. Soc. Jpn. **47**, 1125 (1979).
[24]G. P. Carver, Phys. Rev. B **2**, 2284 (1970).
[25]E. Cartier, F. Heinrich, P. Pfluger, and H.-J. Güntherodt, Solid State Commun. **38**, 985 (1981).
[26]J. Conard, H. Estrade, P. Laguinie, H. Fuzellier, G. Furdin, and R. Vasse, Physica (Utrecht) **99B**, 521 (1980).
[27]H. Zabel and A. Magerl, Phys. Rev. B **25**, 2463 (1982).
[28]S. Funahashi, T. Kondow, and M. Izumi, Solid State Commun. **44**, 1515 (1982).
[29]C. Horie, M. Maeda, and Y. Kuramoto, Physica (Utrecht) **99B**, 430 (1980).
[30]K. Sugihara (private communication).
[31]Y. Koike, H. Suematsu, K. Higuchi, and S. Tanuma, Solid State Commun. **27**, 623 (1978).
[32]Y. Koike, S. Tanuma, H. Suematsu, and K. Higuchi, J. Phys. Chem. Solids **41**, 1111 (1980).
[33]M. Kobayashi and I. Tsujikawa, J. Phys. Soc. Jpn. **46**, 1945 (1979).
[34]M. Kobayashi and I. Tsujikawa, Physica (Utrecht) **105B**, 439 (1981).
[35]M. Kobayashi and I. Tsujikawa, J. Phys. Soc. Jpn. **50**, 3245 (1981).
[36]W. L. McMillan, Phys. Rev. **167**, 331 (1968).
[37]M. Kobayashi (private communication).
[38]M. Kobayashi, T. Enoki, H. Inokuchi, M. Sano, A. Sumiyama, Y. Oda, and H. Nagano, J. Phys. Soc. Jpn. **54**, 2359 (1985).
[39]Y. Takada, J. Phys. Soc. Jpn. **51**, 63 (1982).
[40]R. Al-Jishi, Phys. Rev. B **28**, 112 (1983).